

Diquark Bose-Einstein Condensation and Nuclear Matter

A. H. Rezaeian¹ and H. J. Pirner²

*Institute for Theoretical Physics, University of Heidelberg, Philosophenweg 19,
D-69120 Heidelberg, Germany*

Abstract

We study a possible transition between symmetric nuclear matter and the diquark Bose-Einstein condensate (BEC) matter at zero temperature. We find that chiral restoration transition is first order and coincides with deconfinement. We investigate various possible coexistence patterns which may emerge from the first order deconfinement phase transition by assuming different values for the critical deconfinement chemical potential. If deconfinement takes place at higher chemical potential, there exists a mixed phase of nuclear and chirally restored diquark BEC matter. This coexistence region extends over a large density region for a bigger diquark BEC or a weaker diquark-diquark interaction. For model parameters with heavy diquark in vacuum, phase transition to diquark matter becomes of second-order. We also show that in the case of precocious deconfinement, droplets of nucleons and droplets of chirally restored Bose-Einstein condensed diquarks coexist surrounded by non-trivial vacuum. We show that a early deconfinement and a weak repulsive diquark-diquark interaction soften the equation of state. We propose a scenario in which nuclear matter saturates due to the formation of the diquark BEC and deconfinement phenomena. In this picture, instead of repulsive vector-meson exchange the compressibility of the equation of state is related to a repulsive diquark-diquark interaction. In general, we emphasize the importance of a diquark BEC phase at rather low density before quark BCS-pairing transition.

PACS: 12.38.Mh; 21.65.+f; 12.39.Ki; 24.85.+p

Keywords: Diquark Bose-Einstein condensate; nuclear matter; deconfinement; chiral restoration; quark matter

¹ E-mail: Rezaeian@tphys.uni-heidelberg.de

² E-mail: pir@tphys.uni-heidelberg.de

1 Introduction

Exploring the phases of nuclear and quark matter has recently been subject of intensive investigation both theoretically and experimentally. The phase structure of QCD is relevant for a variety of phenomena, from heavy-ion collisions to neutron stars and the early universe. In particular, such studies may reveal the existence of matter in a new state which may be described by the elementary fields of QCD, i.e. quarks and gluons.

One of the most interesting question in QCD phase diagram is to find the phase boundary between the hadronic and quark phases. It has been well documented that at zero baryonic density, chiral restoration and deconfinement phase transition occur at the same temperature [1]. Our current understanding of QCD phase structure at finite density is still rudimentary. Ab initio lattice Monte-Carlo simulation cannot be directly used due to the complexity of the sampling weight, the so-called sign problem. On the other hand, there is no alternative approach to accommodate all relevant non-perturbative features of QCD and describe both phases in a unified way. Various lattice simulation techniques have recently been proposed in order to circumvent the lattice sign problem (for a recent review see Ref. [2]). But all of them still suffer from systematic uncertainties which made them reliable at very low chemical potential. At low temperature and large densities, a number of model calculations appear to agree on a first order phase transition between nuclear and quark matter [3,4]. Therefore, one expects that a first order phase transition at finite density will end in a second order endpoint and then turns into a rapid crossover at small chemical potential [2]. If confirmed, this indicates that as we approach to lower temperature and finite baryonic density, the phase transition becomes stronger.

At the nuclear matter saturation point the Fermi momentum k_F and the pion mass m_π are of comparable scale $k_F \approx 2m_\pi \approx 260$ MeV. This implies that at the densities of interest in nuclear physics $\rho_0 = 0.15 \text{ fm}^{-3} = 0.45 m_\pi^3$, pions and chiral dynamics must be important. The methods of chiral perturbation theory exploit this observation and have been successful to describe the nuclear matter properties [5]. By estimating the volume occupied by a single nucleon from its mean square charge radius $r_{\text{rms}} = \sqrt{\langle r^2 \rangle}$, one may conclude that baryonic matter is dilute up to about $3\rho_0$, since it can satisfy the diluteness condition $r_{\text{rms}}\rho^{1/3} \ll 1$. At higher density nucleons start to overlap. Nuclear matter is dilute and at the same time it is strongly correlated since $a\rho^{1/3} \gg 1$, where a is the scattering length. On the other hand, since the Fermi momentum exceeds the QCD scale parameter $\Lambda_{\text{QCD}} \approx 200$ MeV, multiple scattering between nucleons on the Fermi surface start to probe distance of the order ≈ 1 fm and the nucleonic substructure becomes visible. The Fermi momentum at saturation point is in fact of the order of $k_F \approx \Lambda_{\text{QCD}}$. The confinement scale can

even become one order of magnitude smaller at moderate baryonic density [6]. Therefore, it is legitimate to ask whether confinement and nuclear matter saturation mechanisms are interconnected. The delta-nucleon mass splitting $\Delta \approx 290$ MeV is also comparable to the Fermi momentum k_F at nuclear matter saturation. It is known that the main mechanism behind the delta-nucleon mass splitting is related to their different internal diquark configurations [8]. Namely, the delta is made of only axial vector diquarks while nucleons can be constructed from both the scalar and axial vector diquarks. This indicates that perhaps diquark dynamics at nuclear matter saturation point might be also relevant. The relevance of diquarks as an efficient way to incorporate the non-perturbative feature of QCD and to simplify the underlying dynamics has been well-known for years (cf. [7,8] and references therein). For example, baryons properties in vacuum have been successfully described in the covariant diquark-quark picture [8]. Recently, it has also been shown that nuclear matter properties can be described by simulating the nucleons as relativistic bound states of the diquarks and quarks [9,10]. At high density diquark concept is also crucial to describe the color superconductivity phenomenon [11,12]. On the other hand, if diquarks as bound states exist, they can in principle undergo Bose-Einstein condensation since they are bosons. Therefore, it seems to be natural to assume that baryonic matter at some density undergoes phase transition to diquark BEC matter. One of the motivations behind this paper is to explore such a transition.

Based on the above scaling argument, it seems that the most important non-perturbative features of QCD might be involved in the nuclear matter saturation density. In this paper we attempt to address such a possible connection between the nuclear matter saturation properties and chiral restoration and the deconfinement effect at zero temperature. We simulate the quark deconfinement at finite density by allowing that the active degrees of freedom change from nucleons to diquarks at high density. This may lead to a first order deconfinement phase transition, in accordance with indications from earlier studies [3,4]. We calculate the nuclear and diquark equations of state (EoS) at zero temperature. In particular, we will investigate a possible diquark Bose-Einstein condensate at about the nuclear matter density. Our result leads to a non-conventional scenario for the stability of the nuclear matter. We show that the nuclear matter is energetically favored to undergo the diquark BEC phase. We study the emergence of various coexistence patterns by allowing the deconfinement to occur at different critical baryonic chemical potential. We will show that it is possible that: all three transitions chiral restoration, the deconfinement and the liquid-gas transition are coincident at zero-temperature.

This paper is organized as follows: In section 2, we first study the diquark BEC dynamics. In section 3, we introduce the hadronic part of our model and calculate the nuclear and diquark EoS. In sections 4 and 5 we investigate the transition between diquark BEC phase and nuclear matter phase at high

and low baryonic density, respectively. Some concluding remarks are given in section 6.

2 Diquark BEC and spectrum of Goldstone modes

With any weak attractive interaction fermions exhibit superfluidity characterized by an energy gap from the BCS pairing mechanism. (For reviews on color superconductivity, see Refs. [13,14]). However, if the attractive interaction is strong, the fermions can form bound bosonic molecules which condense into the bosonic zero-mode at some critical temperature. This is called Bose-Einstein condensation (BEC). These two different mechanisms are in fact two different physical manifestations with the same order parameter and are expected to be connected by a crossover³. In the weak-coupling region at high density the correlation length between two quarks is bigger than the interquark distance or the pair size. However, one may expect that in strong-coupling region at rather low density due to large pair fluctuations, the correlation length becomes smaller than the pair-size and quark matter undergoes the diquark BEC phase [16]. Therefore, at the density around the deconfinement transition, the diquark bound states may be the relevant degrees of freedom. Here, we are interested in the physics of low density (strong-coupling region) where the BEC phenomenon is more relevant. Therefore, we assume that the diquarks bound states are already formed and we concentrate on Bose-Einstein condensation. The diquark matter has been already studied in Ref. [17] but without taking into account the diquark BEC effect. We use the following Lagrangian density for a diquark field Φ ,

$$\mathcal{L}_d = (\partial_0 + i\mu)\Phi^\dagger(\partial_0 - i\mu)\Phi - (\partial_i\Phi^\dagger)(\partial_i\Phi) - m_d^2\Phi^\dagger\Phi - g(\Phi^\dagger\Phi)^2 + \dots, \quad (1)$$

where μ is the chemical potential with respect to the $U(1)$ charge and m_d denotes the diquark mass. The coupling g gives the repulsive diquark-diquark interaction. We assume that the higher-order scattering terms can be ignored. Φ is a color $\bar{3}$ complex scalar field which represents the diquark degree of freedom,

$$\Phi = \begin{pmatrix} 0 \\ 0 \\ \phi_0 \end{pmatrix} + \frac{1}{\sqrt{2}} \begin{pmatrix} \phi_{11} + i\phi_{12} \\ \phi_{21} + i\phi_{22} \\ \phi_{31} + i\phi_{32} \end{pmatrix}, \quad (2)$$

where the complex diquark fields are parameterized in terms of a possible condensate $\phi_0 = \langle\phi\rangle$ (due to symmetry, the direction of condensate is at our

³ This phenomenon has been experimentally examined in various ultracold gases of fermionic alkali atoms using the Feshbach resonance techniques [15].

disposal) and fluctuating fields $\phi_{\alpha 1}$ and $\phi_{\alpha 2}$ with $\alpha = 1, 2, 3$. We have chosen the diquark condensate to be in $\alpha = 3$ direction. The Lagrangian Eq. (1) possesses a $SU(3) \times U(1)$ global symmetry which spontaneously breaks down to $SU(2) \times U(1)_Q$ in the presence of the condensate. This is exactly the same symmetry pattern which underlies the 2SC phase [13,14]. Having substituted the diquark field parameterization Eq. (2) into Lagrangian Eq. (1), one can represent the diquark Lagrangian \mathcal{L}_d Eq. (1) as a sum of the condensate Lagrangian \mathcal{L}_C , free piece \mathcal{L}_F with effective masses m_1 and m_2 and the effective interaction part \mathcal{L}_I among various modes $\phi_{\alpha 1}$ and $\phi_{\alpha 2}$,

$$\begin{aligned}
\mathcal{L}_d &= \mathcal{L}_C + \mathcal{L}_F + \mathcal{L}_I, \\
\mathcal{L}_C &= \left[(\mu^2 - m_d^2) \phi_0^2 - g \phi_0^4 \right], \\
\mathcal{L}_F &= \frac{1}{2} \phi_{31} \left(\partial^\mu \partial_\mu - m_1^2 \right) \phi_{31} + \frac{1}{2} \phi_{11} \left(\partial^\mu \partial_\mu - m_2^2 \right) \phi_{11} \\
&\quad + \frac{1}{2} \phi_{21} \left(\partial^\mu \partial_\mu - m_2^2 \right) \phi_{21} + \sum_\alpha \left(\frac{1}{2} \phi_{\alpha 2} \left(\partial^\mu \partial_\mu - m_2^2 \right) \phi_{\alpha 2} \right. \\
&\quad \left. + \mu \left[\phi_{\alpha 2} \frac{\partial \phi_{\alpha 1}}{\partial t} - \phi_{\alpha 1} \frac{\partial \phi_{\alpha 2}}{\partial t} \right] \right), \\
\mathcal{L}_I &= -\sqrt{2} \left[m_d^2 - \mu^2 + 2g\phi_0^2 + g \sum_\alpha (\phi_{\alpha 1} \phi_{\alpha 1} + \phi_{\alpha 2} \phi_{\alpha 2}) \right] \phi_0 \phi_{31} \\
&\quad - \frac{g}{4} \left(\sum_\alpha (\phi_{\alpha 1} \phi_{\alpha 1} + \phi_{\alpha 2} \phi_{\alpha 2}) \right)^2, \tag{3}
\end{aligned}$$

with

$$\begin{aligned}
m_1^2 &= -\mu^2 + m_d^2 + 6g\phi_0^2, \\
m_2^2 &= -\mu^2 + m_d^2 + 2g\phi_0^2. \tag{4}
\end{aligned}$$

The inverse of free diquark propagator corresponding to Lagrangian Eq. (3) is a 2×2 matrix in $(\phi_{\alpha 1}, \phi_{\alpha 2})$ space for different color directions, and in momentum space it reads

$$\begin{aligned}
i\mathcal{D}_1^{-1}(\omega, p) &= i\mathcal{D}_2^{-1}(\omega, p) = \begin{pmatrix} \omega^2 - p^2 - m_2^2 & 2i\mu\omega \\ -2i\mu\omega & \omega^2 - p^2 - m_2^2 \end{pmatrix}, \\
i\mathcal{D}_3^{-1}(\omega, p) &= \begin{pmatrix} \omega^2 - p^2 - m_1^2 & 2i\mu\omega \\ -2i\mu\omega & \omega^2 - p^2 - m_2^2 \end{pmatrix}. \tag{5}
\end{aligned}$$

The excitation spectrum is found from the diagonalization of the two-point Green function or, equivalently, by solving the conditions $\text{Det}(\mathcal{D}_{\alpha=1,2,3}^{-1}) = 0$. One finds that six degrees of freedom of the complex anti-triplet diquark field

split into a degenerate pair of eigenvalues for $\alpha = 1, 2$ and a singlet pair $\omega_{3\pm}$ for ($\alpha = 3$) (we only consider positive eigenvalues, the negative ones can be treated similarly),

$$\begin{aligned}\omega_{1,2\pm} &= \pm\mu + \sqrt{\mu^2 + p^2 + m_2^2} & (\alpha = 1, 2), \\ \omega_{3\pm} &= \sqrt{p^2 + \frac{1}{2}(m_1^2 + m_2^2) + 2\mu^2 \pm \frac{1}{2}\sqrt{(m_1^2 + m_2^2 + 4\mu^2)^2 + 4(4\mu^2 p^2 - m_1^2 m_2^2)}} & (\alpha = 3).\end{aligned}\quad (6)$$

It is easy to show that in the absence of a condensate $\phi_0 = 0$ the splitting of the three color directions goes away, as it should. For $\mu = 0$ and no symmetry breaking $m_d^2 > 0$ excitation energies are all identical $\omega = \sqrt{k^2 + m_d^2}$ as expected.

The classical potential has a trivial solution $\phi_0 = 0$ and a nontrivial minimum

$$\phi_0^2 = \frac{\mu^2 - m_d^2}{2g}. \quad (7)$$

In the case that $m_d^2 < 0$, symmetry breaking would even occur in vacuum since $\mu^2 - m_d^2$ is then greater than zero. We assume, however, that $m_d^2 > 0$ which means no symmetry breaking at zero baryon density. Only when $\mu^2 > m_d^2$ we have condensation and the trivial $\phi_0 = 0$ is no longer a minimum of potential energy. The system develops an instability with respect to formation of a diquark condensate. In this ground state, the initial $SU(3) \times U(1)$ symmetry spontaneously breaks down to $SU(2) \times U(1)$. Using Eq. (7), the effective masses in Eq. (4) simplify to $m_1^2 = 2(\mu^2 - m_d^2)$ and $m_2 = 0$, and the dispersion relations in Eq. (6) become

$$\begin{aligned}\omega_{1,2\pm} &= \pm\mu + \sqrt{\mu^2 + p^2}, \\ \omega_{3\pm} &= \sqrt{p^2 + 3\mu^2 - m_d^2 \pm \sqrt{(3\mu^2 - m_d^2)^2 + 4\mu^2 p^2}}.\end{aligned}\quad (8)$$

The small momentum expansion of the dispersion relations in far infrared region is given by

$$\omega_{1,2+} \simeq 2\mu + \frac{p^2}{2\mu}, \quad (9)$$

$$\omega_{1,2-} \simeq \frac{p^2}{2\mu}, \quad (10)$$

$$\omega_{3+} \simeq \sqrt{\frac{2(3\mu^2 - m_d^2)^2 + p^2(5\mu^2 - m_d^2)}{3\mu^2 - m_d^2}}, \quad (11)$$

$$\omega_{3-} \simeq \sqrt{\frac{\mu^2 - m_d^2}{3\mu^2 - m_d^2}} p. \quad (12)$$

From the above relations it is noted that the excitation $\omega_{1,2+}$ and ω_{3+} have gaps identical to 2μ and $\sqrt{6\mu^2 - 2m_d^2}$, respectively. The Nambu-Goldstone (NG) bosons can be identified with excitations which are gapless as their momentum goes to zero. Therefore, there are only 3 gapless NG bosons in the spectrum. Due to symmetry consideration one may expect 5 NG bosons. If the conventional counting of NG bosons would apply, the number of NG bosons N is equal to the number of broken generators. However, as has been previously noticed in Lorentz-noninvariant systems the number of NG-modes can be less than the number of broken generators [18]. A more accurate counting rule is due to the Nielsen-Chadha theorem [19] which states that if n_1 and n_2 are the number of gapless excitations with infrared dispersion laws $\omega_1 \simeq p$ and $\omega_2 \simeq p^2$, respectively, then the number of NG bosons $N \leq n_1 + 2n_2$. Therefore, there is no contradiction since two of three gapless modes Eqs. (10,12) have quadratic dispersion laws for long wavelengths. It is interesting to note that at the BEC phase transition point when $\mu \rightarrow m_d$ we have $\omega_{3-} \simeq \frac{p^2}{2\mu}$, and all three gapless excitations become degenerate with the quadratic dispersion law. Therefore, based on the naive continuity of spectrum on the boundary of phase transition, one might have expected less NG bosons. One should also note that since we have gapless mode with quadratic dispersion laws rather linear, the Landau criterion [20] for superfluidity fails⁴. Dissipationless flow in homogeneous bosonic system is one of the manifestation of the interplaying microscopic interaction and the Bose-Einstein condensation. The question whether a Bose-Einstein condensed diquark gas in a more realistic model really displays the Landau criterion for superfluidity remains to be answered elsewhere.

The thermodynamical potential $\Omega_d(\mu, m_d)$ at diquark chemical potential μ is

⁴ According to the Landau criterion, a fluid moving with group velocity v is superfluid if $v < v_c = \text{Min}(\frac{\omega_i(p)}{p})$ where the minimum is taken with respect to all excitation modes and the momentum p . If system has a quadratic dispersion of the low-energy excitation modes, then $v_c = 0$, and Landau criterion can not be satisfied.

obtained through the partition function \mathcal{Z}

$$\Omega_d(\mu, m_d) = i \frac{\ln \mathcal{Z}}{V}, \quad \mathcal{Z} = \int \mathcal{D}\Phi^\dagger \Phi e^{i \int d^4x \mathcal{L}_d}, \quad (13)$$

where V denotes the spacetime volume of the system. The one-loop contribution to the effective potential evaluated at the classical minimum Eq. (7) is obtained as

$$\begin{aligned} \Omega_d(\mu, m_d) &= \Omega_d^{MF} - \frac{1}{2}i \int \frac{d\omega}{2\pi} \int \frac{d^3p}{(2\pi)^3} \left[2 \ln \text{Det } i\mathcal{D}_1^{-1}(\omega, p) + \ln \text{Det } i\mathcal{D}_3^{-1}(\omega, p) \right], \\ &= -\frac{1}{4g}(\mu^2 - m_d^2)^2 + \frac{1}{2} \int \frac{d^3p}{(2\pi)^3} [2(\omega_{1+} + \omega_{1-}) + \omega_{3+} + \omega_{3-}], \end{aligned} \quad (14)$$

where $\mathcal{D}_{1,3}^{-1}$ is defined in Eq. (5) and evaluated at the minimum of the classical action. The $\omega_{1,3\pm}$ is defined in Eq. (8). In the second line in the above equation, we have performed the integration over energy using contour integration. The first term Ω_d^{MF} in Eq. (14) is the mean-field thermodynamical potential evaluated at the minimum of the classical action. The momentum loop-integrals in the diquark effective potential Eq. (14) are divergent and have to be regularized. For simplicity we use a sharp cutoff Λ_D in three-dimensional momentum space. Note that scalar field theory given in Lagrangian Eq. (1) is renormalizable (when higher order interaction terms are ignored), therefore any cutoff dependence can be removed by some kind of renormalization scheme. Here, we assume that the model has a natural ultraviolet cutoff which is defined for the validity of the model at high-energy. We will investigate the implication of various choices for the cutoff.

One can show that the zeroth and first-order derivatives of the thermodynamical potential Eq. (14) with respect to chemical potential μ at $\mu = m_d$ are continuous, but the second-order derivative at $\mu = m_d$ is discontinuous. This indicates a second-order phase transition between normal and diquark condensate phases. The charge density ρ and the speed of sound v_s can be obtained from the thermodynamical potential

$$\rho(\mu) = -\frac{\partial \Omega_d}{\partial \mu}, \quad (15)$$

$$v_s^2 = \frac{\rho}{\mu} \frac{\partial \mu}{\partial \rho}. \quad (16)$$

Using the above relation, the speed of sound at mean-field approximation is

obtained from the first term in the thermodynamical potential Eq. (14),

$$v_s^2 = \sqrt{\frac{\mu^2 - m_d^2}{3\mu^2 - m_d^2}}. \quad (17)$$

Note also that this is identical to the coefficient of ω_{3-} in Eq. (12). At very high density $\mu \gg m_d$ we recover the standard relativistic result $v_s = \frac{1}{\sqrt{3}}$ independent of the model parameters. This indicates that at very high density the NG boson propagates as in a relativistic medium.

3 Diquark BEC and the nuclear matter equation of state

We incorporate the deconfinement effect by allowing that the active degrees of freedom change from baryons to diquarks at a critical baryonic critical chemical potential μ_b^* . For description of the hadronic phase, we use the chiral $\sigma - \omega$ model with exact global $SU(2) \times SU(2)$ symmetry, which contains a pseudoscalar coupling between pions and massive isoscalar vector field ω^μ to nucleons,

$$\begin{aligned} \mathcal{L}_h = & \bar{\psi}_n [\gamma_\mu (i\partial^\mu - g_{vn}\omega^\mu) - g_n (\sigma + i\gamma_5 \vec{\tau}\vec{\pi}) + \mu_b \gamma_0] \psi_n - \frac{1}{4} F_{\mu\nu} F^{\mu\nu} \\ & + \frac{1}{2} g_v^2 \omega^\mu \omega_\mu (\sigma^2 + \vec{\pi}^2) + \mathcal{L}_{\sigma\pi}, \end{aligned} \quad (18)$$

$$\mathcal{L}_{\sigma\pi} = \frac{1}{2} (\partial_\mu \sigma \partial^\mu \sigma + \partial_\mu \vec{\pi} \partial^\mu \vec{\pi}) + \frac{m_s^2}{2} (\sigma^2 + \vec{\pi}^2) + \frac{\lambda}{4} (\sigma^2 + \vec{\pi}^2)^2, \quad (19)$$

where the field tensor is defined $F_{\mu\nu} = \partial_\mu \omega_\nu - \partial_\nu \omega_\mu$ and μ_b denotes the baryonic chemical potential. The nucleon mass M_N and the vector-meson mass m_v at rest are generated through spontaneous symmetry breaking by the σ -field

$$M_N(\sigma) = g_n \sigma, \quad m_v(\sigma) = g_v \sigma. \quad (20)$$

The energy density for the hadronic phase can be obtained from Eq. (19) in the conventional mean-field approximation. Having used the equation of motion for the ω^0 field, we obtain the energy density as

$$\begin{aligned} \varepsilon_h = & V(\bar{\sigma}) + \frac{g_{vn}^2 \rho_b^2}{2m_v^2(\bar{\sigma})} + \frac{2}{\pi^2} \int_0^{k_F} dk \, k^2 \omega_N(k, \bar{\sigma}) \\ & - \frac{2}{\pi^2} \int_0^{\Lambda_N} dk \, k^2 (\omega_N(k, \bar{\sigma}) - \omega_N(k, \bar{\sigma}_0)), \end{aligned} \quad (21)$$

$$V(\bar{\sigma}) = \frac{m_s^2}{2} (\bar{\sigma}^2 - \bar{\sigma}_0^2) + \frac{\lambda}{4} (\bar{\sigma}^4 - \bar{\sigma}_0^4) \quad (22)$$

where we defined $\omega_N(k, \bar{\sigma}) = \sqrt{k^2 + M_N^2(\bar{\sigma})}$ and $\bar{\sigma}$ (and $\bar{\sigma}_0$) denotes the mean-value of the sigma field in the nuclear matter medium (and in the vacuum). We have also included the corresponding Dirac-sea of the nucleon up to a ultraviolet cutoff Λ_N . In principle, in renormalizable models such as the linear sigma model, divergences can be absorbed into the coefficient of interaction terms by employing a renormalization scheme. However, it has been shown that for this kind of models with heavy fields, such terms give rise to unnaturality⁵ indicating that quantum vacuum is not adequately described by long-range degrees of freedom [21]. We have recently shown that nuclear matter properties can be better reproduced if one treats the vacuum loop explicitly [24]. We discard the short-range physics which cannot be described by long-range degrees of freedom by the nucleonic ultraviolet cutoff Λ_N . The baryonic density ρ_b is related to the Fermi momentum k_F by

$$\rho_b = \frac{2}{\pi^2} \int_0^{k_F} dk k^2 = \frac{2k_F^3}{3\pi^2}. \quad (23)$$

At any density ρ_b , ε_h is stationary with respect to the mean-value of the scalar field. Therefore, the scalar mean-field $\bar{\sigma}$ is obtained via the self-consistency conditions:

$$\frac{d\varepsilon_h}{d\bar{\sigma}} = 0. \quad (24)$$

This equation is numerically solved for every point of density. The baryonic chemical potential μ_b can be obtained through the Hugenholtz-van Hove theorem via the energy density

$$\mu_b = \frac{\partial \varepsilon_h}{\partial \rho} = \frac{g_{vn}^2 \rho_b}{m_v^2(\bar{\sigma})} + \omega_N(k_F, \bar{\sigma}), \quad (25)$$

where the value of $\bar{\sigma}$ for a given density is obtained via Eq. (24). Then the thermodynamical potential Ω_h and the hadronic pressure P_h are obtained through a Legendre transformation and can be written as

$$\begin{aligned} \Omega_h = -P_h = \varepsilon_h - \mu_b \rho_b = V(\bar{\sigma}) - \frac{g_{vn}^2 \rho_b^2}{2m_v^2(\bar{\sigma})} \\ + 4 \int \frac{d^3k}{(2\pi)^3} \left(\omega_N(k, \bar{\sigma}) + \frac{g_{vn}^2 \rho_b}{m_v^2(\bar{\sigma})} - \mu_b \right) \Theta \left(\mu_b - \omega_N(k, \bar{\sigma}) - \frac{g_{vn}^2 \rho_b}{m_v^2(\bar{\sigma})} \right) \\ - \frac{2}{\pi^2} \int_0^{\Lambda_N} dk k^2 (\omega_N(k, \bar{\sigma}) - \omega_N(k, \bar{\sigma}_0)). \end{aligned} \quad (26)$$

⁵ Furnstahl *et. al.* [21] have shown that the one-baryon-loop vacuum contribution in renormalized models like the linear sigma model and the Walecka model gives rise to large *unnatural* coefficients based on the “naive dimensional analysis” proposed by Georgi and Manohar [22].

For the deconfined phase we consider matter made of diquarks coupled to σ and $\vec{\pi}$ and we use the diquark Lagrangian introduced in the previous section. The new input here is that we couple the diquark field to the scalar field in order to generate the diquark mass dynamically via spontaneous symmetry breaking.

$$\mathcal{L}_q = (\partial_0 + i\mu)\Phi^\dagger(\partial_0 - i\mu)\Phi - (\partial_i\Phi^\dagger)(\partial_i\Phi) - (g_d\sigma)^2\Phi^\dagger\Phi - g(\Phi^\dagger\Phi)^2 + \mathcal{L}_{\sigma\pi}. \quad (27)$$

The Lagrangian $\mathcal{L}_{\sigma\pi}$ is defined in Eq. (19). We incorporate the diquark BEC effect in the fashion presented in the previous section, namely by employing the diquark field parametrization Eq. (2). We treat the diquark fields at the one-loop level. Therefore, the thermodynamical potential Ω_q and deconfined pressure P_q are given by

$$\Omega_q = -P_q = \Omega_d(\mu, m_d(\bar{\sigma})) + V(\bar{\sigma}) - \frac{3}{2\pi^2} \int_0^{\Lambda_D} k^2 dk \sqrt{k^2 + m_d^2(\bar{\sigma}_0)}, \quad (28)$$

where the diquark mass is related to the σ -field:

$$m_d(\sigma) = g_d\sigma. \quad (29)$$

The Ω_d and $V(\bar{\sigma})$ in Eq. (28) are defined in Eqs.(14) and (22), respectively. The last term in Eq. (28) is the constant diquark contribution at zero density which shifts the minimum of the vacuum thermodynamical potential to zero. Note that the diquark mass now dynamically changes in medium through the in-medium σ -field. This does not alter the possible formation of the diquark BEC as far as $\mu^2 > m_d^2$ where μ is the diquark chemical potential. In contrast to the Bag model and similarly to the NJL model, our diquark model dynamically generates a density-dependent bag constant and density dependent effective constituent diquark masses. With the diquark thermodynamical potential Eq. (28) and the density Eq. (15) one can construct the energy density through the Legendre transformation,

$$\begin{aligned} \varepsilon_q = \Omega_q + \mu\rho(\mu) = & V(\bar{\sigma}) + \frac{1}{4g} (\mu^2 - m_d^2(\bar{\sigma})) (3\mu^2 + m_d^2(\bar{\sigma})) \\ & + \frac{1}{\pi^2} \int_0^{\Lambda_D} \frac{p^4 dp}{\sqrt{p^2 + \mu^2}} \\ & + \frac{1}{2\pi^2} \int_0^{\Lambda_D} p^2 dp \left(\frac{(p^2 - m_d^2(\bar{\sigma})) \omega_{3+}\omega_{3-} + \omega_{3+}^2\omega_{3-}^2 - p^2\mu^2}{\omega_{3+}\omega_{3-}(\omega_{3+} + \omega_{3-})} \right) \\ & - \frac{3}{2\pi^2} \int_0^{\Lambda_D} k^2 dk \sqrt{k^2 + m_d^2(\bar{\sigma}_0)}, \end{aligned} \quad (30)$$

where for the right hand side we have made use of the definition of $\rho(\mu)$ and Ω_q given in Eqs. (15,28). The $\omega_{3\pm}$ and $V(\bar{\sigma})$ are defined in Eqs. (8) and (22), respectively. Using Eq. (8) we obtain the following relations which facilitate the computation

$$\begin{aligned}\omega_{3+}\omega_{3-} &= p\sqrt{p^2 + 2(\mu^2 - m_d^2(\bar{\sigma}))}, \\ \omega_{3+} + \omega_{3-} &= \sqrt{2}\sqrt{p^2 + 3\mu^2 - m_d^2(\bar{\sigma})} + p\sqrt{p^2 + 2(\mu^2 - m_d^2(\bar{\sigma}))}.\end{aligned}\quad (31)$$

The in-medium mean-value of the scalar field and the corresponding diquark mass is obtained similarly to the hadronic sector by minimization

$$\frac{d\varepsilon_q}{d\bar{\sigma}} = 0. \quad (32)$$

The diquark chemical potential and density (μ, ρ) are related to baryonic ones (μ_b, ρ_b) by: $\mu = \frac{2}{3}\mu_b$ and $\rho = \frac{3}{2}\rho_b$. The binding energy per baryon is defined as

$$\frac{E_B}{A} = \frac{\varepsilon_{h,q}}{\rho_b} - M_N(\bar{\sigma}_0) = -\frac{P_{h,q}}{\rho_b} + \mu_b - M_N(\bar{\sigma}_0), \quad (33)$$

where $\varepsilon_{h,q}$ and $p_{h,q}$ are defined in Eqs. (21,30) and Eqs. (26,28), respectively.

4 Nuclear-diquark phase transition at high density

We incorporate the deconfinement effect by demanding that as we increase the density in the hadronic phase at a critical Fermi momentum k_F^* corresponding to the baryonic chemical potential μ_b^* , the baryonic degrees of freedom are replaced by diquark ones while keeping the description of the auxiliary scalar fields intact above the transition. We do not couple the vector-meson field to diquarks. The exact value of the deconfinement chemical potential μ_b^* is not known. Therefore, we will consider the implication of different choices for μ_b^* and k_F^* .

In the hadronic phase, our model contains six unknown parameters Λ_N , m_s^2 , λ , g_n , g_{vn} and g_v . We take the hadronic ultraviolet cutoff $\Lambda_N = 324$ MeV [24]. In this model the acceptable range of the ultraviolet cutoff Λ_N is rather low [24]. This empirical fact has been also observed by other authors within the NJL model with nucleonic degrees of freedom [25]. This is in contrast with the case that the model is defined in terms of quark degrees of freedom where the allowed range of the cutoff is typically larger. Due to spontaneous symmetry breaking the scalar mean field acquires a nonzero vacuum expectation value which is equal to the pion decay. The pions are then the massless Nambu-Goldstone bosons. For the given $\Lambda_N = 324$ MeV, one can determine the scalar potential couplings m_s^2 and λ so that the mean-value of the scalar field becomes identical to the empirical pion decay at vacuum $\bar{\sigma}_0 = 93$ MeV. We take the empirical nucleon mass in vacuum $M_N(\bar{\sigma}_0) = 939$ MeV and vector-meson mass in vacuum $m_v(\bar{\sigma}_0) = 783$ MeV. These choices fix the coupling $g_n = M_N/f_\pi = 10.1$ and $g_v = m_v/f_\pi = 8.42$. The vector coupling g_{vn} is treated

parameter	$\Lambda_N(\text{MeV})$	$m_s^2(\text{GeV}^2)$	λ	g_{vn}	g_n	g_v
set NM	324	+0.026	25	6.54	10.1	8.42

Table 1

The value of various couplings in hadronic phase for set NM is given. This parameter set reproduces the empirical saturation point ($E_b/A = -15.75$ MeV, $\rho_0 = 0.15 \text{ fm}^{-3}$).

as a free parameter and is adjusted in the medium in such a way that the EoS reproduces nuclear-matter saturation properties, namely a binding energy per nucleon $E_B/A = -15.75$ MeV at a density corresponding to a Fermi momentum of $k_F = 256 \text{ MeV} = 1.3 \text{ fm}^{-1}$ [23]. In this way all parameters in the confined phase are fixed uniquely (see set NM in table 1).

The sigma mass can be obtained from

$$m_\sigma^2 = \frac{\partial^2 \Omega_h}{\partial \bar{\sigma}^2}, \quad (34)$$

where the derivatives are evaluated at the scalar mean-field $\bar{\sigma}$ solution of the gap equation. The corresponding sigma meson mass m_σ in vacuum for the above parameters (set NM in table 1) is 810 MeV. In order to estimate the stiffness of the nuclear matter EoS, one may compute the compression modulus at the saturation density. It is defined as

$$K = -9 \frac{d\Omega_h}{d\rho_b} = 9\rho_b \frac{\partial^2 \varepsilon_h}{\partial \rho_b^2}. \quad (35)$$

The compression modulus at saturation density for the parameter set NM is $K = 455$ MeV. Note that in the original $\sigma-\omega$ model of Boguta the compression modulus of nuclear matter is unacceptably large about $K = 650$ MeV [26]. Here, due to the inclusion of the Dirac-sea we are relatively able to reduce the compression modulus (see also Ref. [24]). This value is still bigger than the empirical one which is believed to be about $K = 200 - 300$ MeV [28,29]. Nevertheless, here we use only the nuclear matter compression modulus as a relative measure of stiffness of the deconfined EoS. It has been very difficult to overcome the unphysically high values of compressibility in the $\sigma-\omega$ model and in the Walecka model. In the next section we will introduce a non-conventional scenario in which the nuclear matter compressibility can be lowered.

For zero temperature, two phases of hadrons and diquarks can be in equilibrium if their chemical potentials and pressures are equal (Gibbs' conditions):

$$P_q(\mu_b^*) = P_h(\mu_b^*), \quad \frac{3}{2}\mu = \mu_b = \mu_b^*, \quad (36)$$

where P_h and P_q are defined in Eqs. (26) and (28), respectively. First, we assume that the transition to the diquark BEC matter occurs at the baryonic

Parameter ($\mu_b^* = 1214.5$ MeV)	set A1	set A2	set A3	set A4
g	14.1	13.47	12.73	11.23
g_d	6.85	6.7	6.5	6.0
$m_d(\rho = 0)(\text{MeV})$	637.1	623.1	604.5	558.0
ρ_b^h/ρ_0	3.0	3.0	3.0	3.0
ρ_b^d/ρ_0	3.0	4.0	5.4	8.6

Table 2

The parameters g_d and g in the deconfined phase for the sets A1-A4 for the critical deconfinement chemical potential $\mu_b^* = 1214.5$ MeV. We assume as ultraviolet cutoff for all parameter sets $\Lambda_D = 900$ MeV. The baryonic density at the transition point in hadronic ρ_b^h and diquark ρ_b^d parts in units of the normal nuclear matter density $\rho_0 = 0.15 \text{ fm}^{-3}$ are also given.

chemical potential $\mu_b^* = 1214.5$ MeV which corresponds to the baryonic density $\rho_b^h = 3\rho_0$ from the hadronic side. For the deconfined phase, we have three unknown parameters: the ultraviolet cutoff Λ_D , the diquark-diquark coupling g and the diquark-scalar field coupling g_d . We assume the deconfined ultraviolet cutoff to be $\Lambda_D = 900$ MeV and fix the other two unknown parameters by Gibbs' conditions Eq. (36). We require that at the phase transition the baryonic chemical potential of both hadronic and diquark parts to be equal $\mu_b = \frac{3}{2}\mu = \mu_b^* = 1214.5$ MeV. Having obtained the nuclear matter EoS, one can immediately read off the hadronic pressure at the critical deconfinement chemical potential: $P_h(\mu_b^* = 1214.5 \text{ MeV}) = 89.8 \text{ MeV/fm}^3$. Therefore, the Gibb's condition for equilibrium of two phases is satisfied if $P_h(\mu_b^*) = P_q(\mu_b^*) = 89.8 \text{ MeV/fm}^3$. This gives a non-trivial constraint on the diquark-model parameters. There exist many solutions which satisfy the above requirements, each of them corresponds to a different BEC condensate. The values of parameters g and g_d for four sets A1-A4 with a fixed $\Lambda_D = 900$ MeV are given in table 2. We have also given in table 2 the value of the diquark mass in vacuum using Eq. (29). Note that the values of the scalar diquark mass in vacuum for various parameter sets given in table 2 is within the acceptable range which has been estimated by many authors in order to describe the baryon properties in vacuum [8,7,27].

In Fig. 1, we show the mean-value of the scalar field $\bar{\sigma}$ with respect to the baryonic chemical potential μ_b . The solid line denotes the mean-value of the scalar field in the nuclear matter medium when the deconfinement to diquark matter is not incorporated. For all diquark parameter sets (given in table 2) chiral phase transition takes place at the critical deconfinement chemical potential $\mu_b^* = 1214.5$ MeV. We will show later that this will also be the case if the critical deconfinement chemical potential is taken lower value.

In Fig. 2 (right pannel), we show the diquark pressure P_q for sets A1-A4 (in

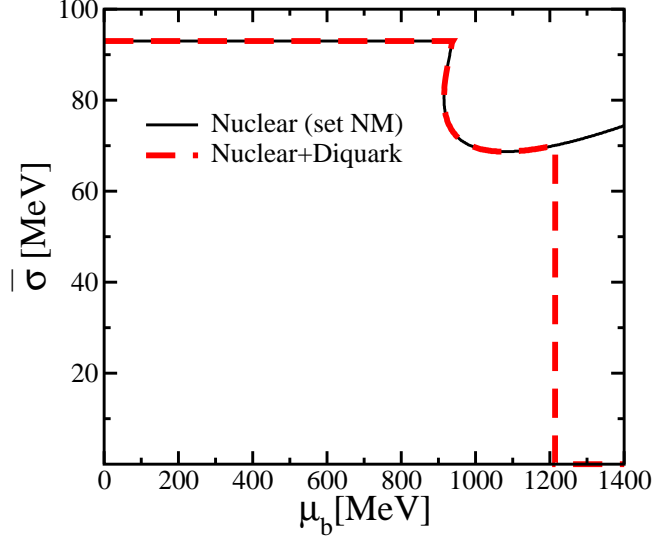


Fig. 1. In-medium pion decay constant $\bar{\sigma}$ as a function of baryonic chemical potential μ_b . We use the parameter set NM given in table 1 for nuclear matter and parameter sets A1 – A4 given in table 2 for diquark matter.

table 2) and the hadronic pressure P_h for set NM (in table 1) as a function of the baryonic chemical potential μ_b . For comparison we also display the nuclear matter solution for the parameter set NM when the transition to a diquark BEC is not incorporated. It is obvious that the EoS becomes considerably softer if deconfinement is allowed. Therefore, the system is energetically favored to undergo phase transition. By comparing different diquark EoS obtained by using various parameter sets given in table 2, it is observed that a bigger diquark-diquark coupling g leads to a stiffer EoS, whilst a bigger coupling g leads to a smaller diquark condensate, see Eq. (7). Therefore, the bigger the diquark BEC condensate the softer the EoS will be. The inserted plot in Fig. 2 shows the first-order liquid-gas phase transition of nuclear matter which takes place at $\mu_b = 923.25$ MeV. The first-order phase transition is manifested by the appearance of several branches of $P_h(\mu_b)$. At a fixed baryonic chemical potential, only the highest pressure corresponds to a stable phase. The slope of curves $P(\mu_b)$ exhibits a jump in density. In Fig. 2 (left pannel), we show the baryonic density ρ_b in units of nuclear matter density ρ_0 as a function of the baryonic chemical potential, we have also plotted the critical deconfinement chemical potential μ_b^* . In general, there are two separated density jumps with respect to the chemical potential: one corresponds to the standard nuclear matter liquid-gas phase transition and the second one corresponds to the deconfinement phase transition. The value of baryonic density below and above deconfinement is given in table 2. Depending on model parameters the jump at the deconfinement transition can change. The softest EoS set A4 results in a high baryonic density above the phase transition since the diquark BEC condensate is bigger and consequently it can accommodate more baryon density. Note also that the set A4 has the lowest diquark mass in vacuum, see table

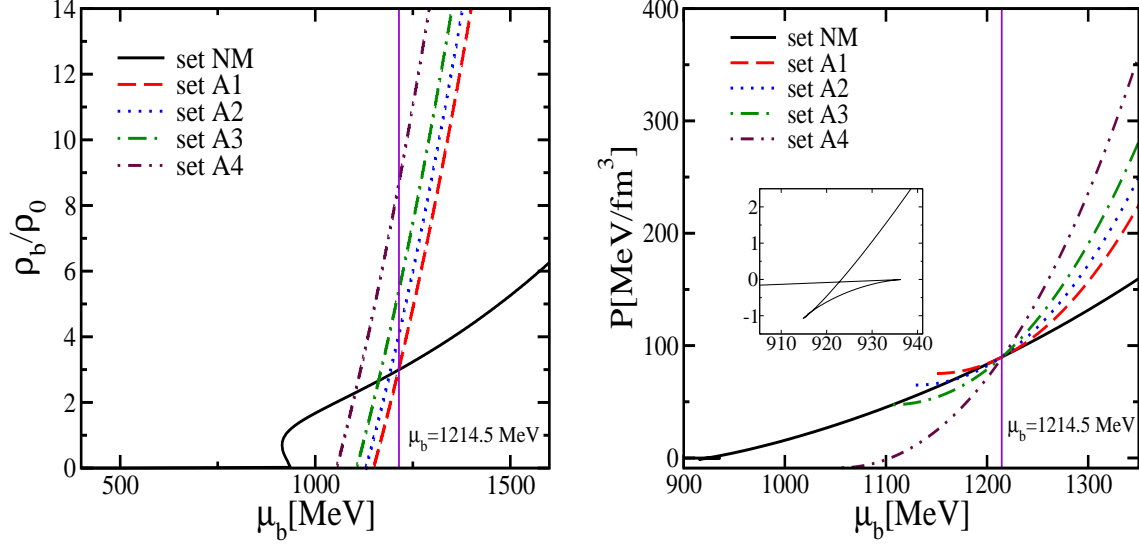


Fig. 2. Baryon number densities (left) in units of nuclear matter density $\rho_0 = 0.15 \text{ fm}^{-3}$ and pressure (right) as functions of the baryonic chemical potential μ_b for various parameter sets given in tables 1 and 2. The critical deconfinement line $\mu_b^* = 1214.5 \text{ MeV}$ is also shown. The insert shows the region of the nuclear matter liquid-gas phase transition.

2. For the model parameter (set A1) with rather heavy diquark in vacuum, transition to diquark matter takes place without a density jump, i. e. the first derivative of the thermodynamical potential with respect to the chemical potential is continuous. This indicates a second-order phase transition between hadronic and diquark matter. In this case, although deconfinement and chiral phase transition coincides, their phase orders are different.

In order to consider the possible coexistence regions which emerge from the first-order phase transition, we perform Maxwell constructions. In Fig. 3, we show the energy per baryon $\varepsilon_{h,q}/\rho_b$ as a function of inverse baryonic density $(\rho_b/\rho_0)^{-1}$ for the parameter set A4 given in table 2. It exhibits a typical Van der Waals-like diagram. Using the following thermodynamical consistency equation and Gibb's conditions,

$$\frac{\partial}{\partial \rho_b^{-1}} \left(\frac{\varepsilon_{h,q}}{\rho_b} \right) = -P_{h,q}, \quad (37)$$

one can identify the coexistence region as a function of inverse density. There exist two separated coexistence regions which are denoted in Fig. 3 as coexistence region 1 and 2. At low density $0 \leq \rho_b \leq \rho_0$ in the hadronic phase we have the typical coexistence between nucleonic gas and nuclear droplet. At rather high density $3\rho_0 \leq \rho_b \leq \rho_b^d$ (for values of ρ_b^d see table 2), there exist a coexistence region between nuclear matter and chirally restored diquark BEC matter. At zero temperature, the coexistence region between the hadronic and diquark BEC phase seems to be quite large in the density axis for a weaker

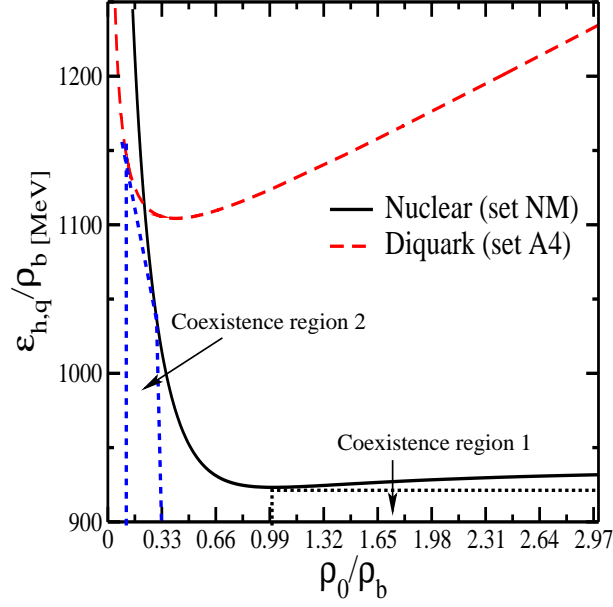


Fig. 3. Energy per baryon number as functions of inverse baryonic density in units of the nuclear matter density, i. e. $(\rho_b/\rho_0)^{-1}$ when the deconfinement chemical potential is taken $\mu_b^* = 1214.5$ MeV. The dotted lines represent the Maxwell-constructions which determine the regions of coexistence. The coexistence region 1 contains the nucleonic gas and nuclear droplets and the coexistence region 2 contains mixed nuclear and diquark BEC matter.

diquark-diquark interaction or a bigger diquark BEC (see parameter set A4). Forcrand *et al.* [32] have recently found some indication for the coexistence region of the hadron and the plasma phases based on the canonical approach of lattice QCD (for 4-flavour and pion mass $m_\pi \approx 350$ MeV). Their extrapolation indicates that the coexistence region might be quite wide in density $0.50(5) \text{ B/fm}^3 \lesssim \rho \lesssim 1.8(3) \text{ B/fm}^3$. It is of great interest to see if this coexistence region will survive in the chiral limit using a fully realistic simulation of QCD.

5 Nuclear-diquark phase transition at low density

In this section, we consider the possibility that the deconfining transition happens at a lower baryonic chemical potential. In particular, we study the extreme case where the deconfinement phase transition takes place right at the nuclear matter saturation Fermi momentum, namely at $k_F^* = 256$ MeV which is approximately equal to the QCD confinement scale Λ_{QCD} . This corresponds to a baryonic chemical potential $\mu_b^* = M_N(\bar{\sigma}_0) - E_B/A = 923.25$ MeV. At the saturation point, the binding energy per nucleon is taken $E_B/A = 15.75$ MeV. Above the deconfinement phase transition the vector-meson does not appear in the deconfined Lagrangian \mathcal{L}_q Eq. (27) and one may be afraid that

Parameter ($\mu_b^* = 923.25$ MeV)	set B1	set B2	set B3	set B4
g	18.16	16.43	15.46	14.34
g_d	4.8	4.56	4.40	4.18
$m_d(\rho = 0)(\text{MeV})$	446.4	424.1	409.2	388.8
ρ_b^h/ρ_0	1.0	1.0	1.0	1.0
ρ_b^d/ρ_0	0.23	1.0	1.6	2.24

Table 3

The parameters g_d and g in the deconfined phase for the sets B1-B4 for the critical deconfinement chemical potential $\mu_b^* = 923.25$ MeV. The diquark ultraviolet cutoff for all parameter sets is taken $\Lambda_D = 650$ MeV.

nuclear matter in this model would collapse [26]. However, we will show that the repulsive diquark interaction induces enough repulsion to reproduce stable matter similar to conventional nuclear matter.

For the case of early deconfinement, a lower diquark ultraviolet cutoff Λ_D is allowed since we are interested in physics of rather low baryonic chemical potential. We assume as diquark ultraviolet cutoff $\Lambda = 650$ MeV. Later we will investigate the effect of choosing a higher value for the ultraviolet cutoff. The acceptable range of the diquark-scalar field coupling g_d and the diquark-diquark coupling g is determined via the Gibb's condition. Since from the hadronic part at the saturation point we have that the hadronic pressure $P_h(\mu_b^*) = 0$, we require that also the diquark pressure $P_q(\mu_b^* = 923.25\text{MeV}) = 0$. In table 3 we give the values of the couplings in four parameter sets B1-B4 obtained by the above-mentioned procedure.

In Fig. 4, we show the in-medium pion decay constant $f_\pi = \bar{\sigma}$ as a function of the baryonic chemical potential μ_b (left pannel) and baryonic density ρ_b/ρ_0 (right pannel). The chiral restoration for all parameter sets given in table 3 is first order and takes place right at the critical deconfinement chemical potential μ_b^* . The solid line denotes the mean-value of the scalar field in the nuclear matter medium without deconfinement effect. It is well known that in the $\sigma - \omega$ model with dynamical ω -mass, chiral restoration does not occur since $\bar{\sigma}$ tends to grow at high density. This can also be seen in Figs. 1 and 4, where $\bar{\sigma}$ at higher chemical potential and density in nuclear medium (solid line) bends upward. In fact this feature of the model is closely connected to the stability of the system. The sigma field plays the role of the chiral partner of the pion and at the same time it is the mediator of medium-range nucleon-nucleon attraction and via the ω -mass also the short range repulsive is related to the sigma field. Therefore, as its mass becomes smaller the attraction between nucleons becomes stronger which may destroy the stability of nuclear matter. This effect is not present in non-chiral type models such as the Walecka model [23]. However, we will show that in our approach the chiral restoration does

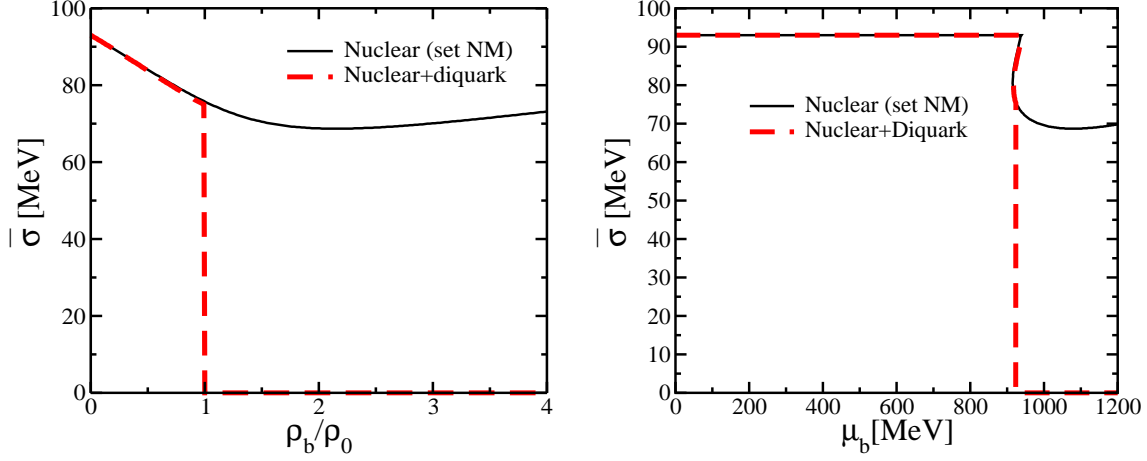


Fig. 4. In-medium pion decay constant $\bar{\sigma}$ as functions of density ρ_b/ρ_0 (left) in unit of nuclear matter density $\rho_0 = 0.15 fm^{-3}$ and baryonic chemical potential μ_b (right). We have used parameter sets NM and set B2 given in tables 1 and 3.

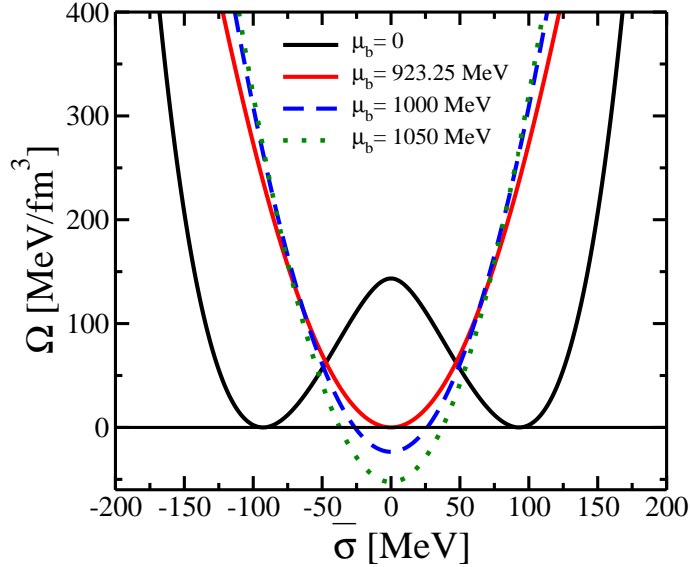


Fig. 5. Thermodynamic potential Ω_q (and Ω_h) as a function of auxiliary variable $\bar{\sigma}$ (pion decay) for parameter set NM (for $\mu_b = 0$) and for other values of μ_b the parameter set B2 is used.

not obstruct the stability of the system.

The thermodynamic potentials Ω_q and Ω_h as a function of the auxiliary variable $\bar{\sigma}$ are shown in Fig. 5. In vacuum the minimum of the thermodynamic potential Ω_h is located at the pion decay $\bar{\sigma} = 93$ MeV. As we increase the chemical potential right at the critical deconfinement chemical potential μ_b^* where we switch to the diquark thermodynamic potential Ω_q , there is a strong first order phase transition from the vacuum to the chirally restored phase with $\bar{\sigma} = 0$. Once the phase transition has taken place, the minimum of Ω_q at $\bar{\sigma} = 0$ remains with increasing chemical potential, but the lowest Ω_q configuration

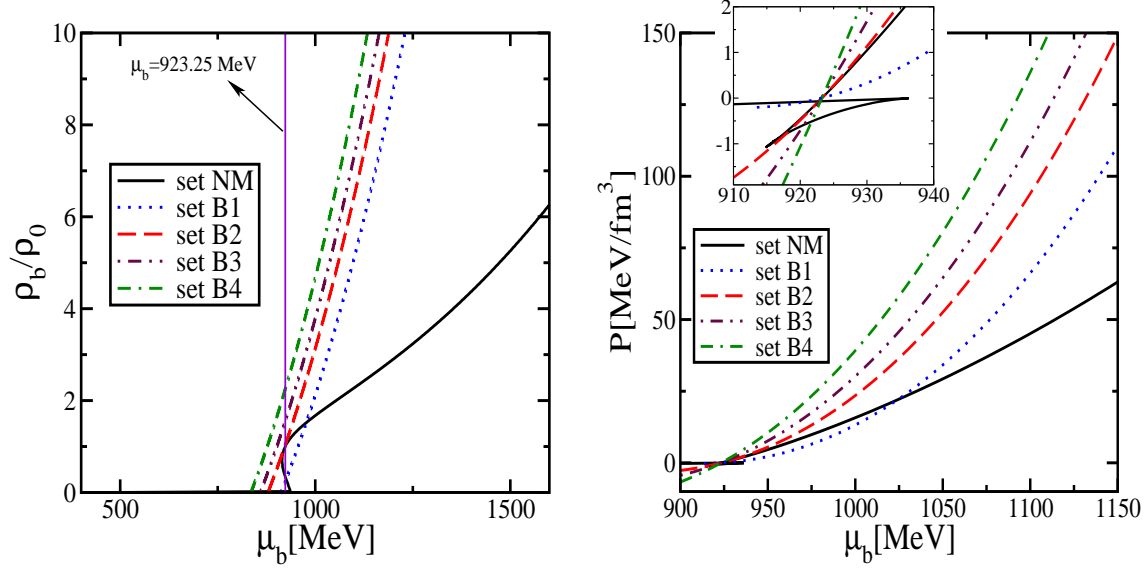


Fig. 6. Baryon number densities (left) in units of nuclear matter density $\rho_0 = 0.15 \text{ fm}^{-3}$ and pressure (right) as functions of the baryonic chemical potential μ_b for various parameter sets given in tables 1 and 3. For comparison we have also plotted the nuclear matter solution (solid line) for the parameter set NM when transition to diquark matter is not taken into account.

becomes more and more negative $\Omega_q < 0$, indicating an increase in pressure $P_q > 0$ with density. At the critical chemical potential $\mu_b^* = 923.25$ MeV, both minima of Ω_h and Ω_q have zero pressure. One represents the non-perturbative broken vacuum at density zero and the other represents the chirally restored diquark BEC phase at non-zero density ρ_b . Note that we construct the deconfinement phase transition in such a way that the chiral phase transition results. The chiral restoration is first order and coincides with the deconfinement critical chemical potential.

In Fig. 6 (right panel), we show the nuclear matter pressure P_h for set NM (in table 1) and the diquark matter pressure P_q for set B1-B4 (in table 3) as a function of the baryonic chemical potential. It is seen that above the critical deconfinement chemical potential the diquark EoS becomes generally softer than nuclear matter solution. As in the previous case (in Fig. 2), the behavior of the diquark EoS depends on the diquark-diquark coupling g and consequently on the strength of the diquark Bose-Einstein condensate. A bigger diquark-diquark coupling g leads to a stiffer EoS. A diquark-diquark coupling g induces enough repulsion in order to prevent the collapse of the system to infinite diquark BEC condensate and makes the system stable. The inserted plot in Fig. 6 shows more clearly the appearance of several branches of $P(\mu_b)$ which is a manifestation of first-order phase transition. At a fixed baryonic chemical potential only the highest positive pressure corresponds to a stable phase. In Fig. 6 (left panel), we show the baryonic density ρ_b/ρ_0 as a function of the baryonic chemical potential μ_b for various parameter sets. The

Parameter ($\mu_b^* = 923.25$ MeV)	set B2	set C	set D
Λ_D (MeV)	650	750	900
g	16.43	11.64	7.48
g_d	4.56	4.85	5.1
$m_d(\rho = 0)$ (MeV)	424.1	451.1	474.3

Table 4

The parameters Λ_D , g_d and g in the deconfined phase of the model when the critical deconfinement chemical potential $\mu_b^* = 923.25$ MeV is assumed. Parameter set B2 is already given in table 3. All parameter sets lead to baryonic density $\rho_b^h = \rho_0$ at the critical deconfinement chemical potential $\mu_b^* = 923.25$ MeV and reproduce the empirical saturation point ($E_b/A = -15.75$ MeV, $\rho_0 = 0.15$ fm³).

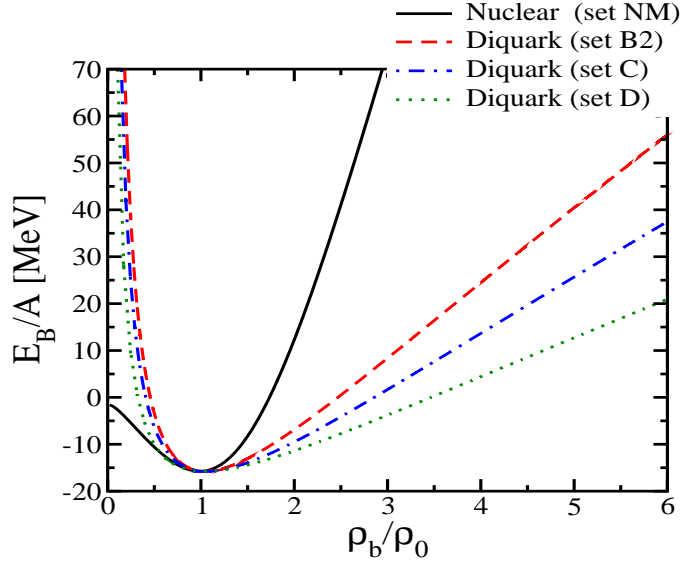


Fig. 7. The binding energy per baryon E_B/A as a function of density ρ_b/ρ_0 for the nuclear matter with parameter set NM (table 1) and for the diquark matter with different diquark ultraviolet cutoff Λ_D given in table 4.

deconfinement phase transition leads to a baryonic density jump at the critical chemical potential $\mu_b^* = 923.25$ MeV similarly to the nuclear matter liquid-gas phase transition. In this case, the deconfinement transition can only be first-order since in hadronic side, the pressure has multi-branches.

In order to understand the implication of different choices for the diquark ultraviolet cutoff Λ_D , we also calculated the diquark EoS for three different values of the cutoff Λ_D given in table 4, assuming that the deconfinement takes place at $\mu^* = 923.25$ MeV. All parameter sets given in table 4 reproduced the empirical saturation point ($E_b/A = -15.75$ MeV, $\rho_0 = 0.15$ fm³). It is seen from table 4 that by increasing the cutoff Λ_D , a weaker repulsive diquark-diquark coupling g is needed. In Fig. 7, we show the binding en-

ergy per baryon for the hadronic matter with parameter set NM (in table 1) and for diquark matter with various parameter sets given in table 4. For all diquark parameter sets in table 4, at the critical deconfinement chemical potential μ_b^* the baryonic density is equal to the normal nuclear matter density $\rho_b^d = \rho_0 = 0.15 \text{ fm}^{-3}$. It is obvious that at high density diquark matter is energetically favored compared with nuclear matter while at low density nuclear matter is the stable one. Note the EoS of the hadron or the diquark EoS alone has a minimum at the saturation density since we have $P_h = P_q = 0$ at $\mu_b^* = 923.25 \text{ MeV}$, reflecting the thermodynamical consistency equation (37). The produced nuclear-diquark EoS is softer than the pure nuclear matter EoS⁶. By lowering the diquark ultraviolet cutoff Λ_D , the diquark EoS becomes stiffer, see Fig. 7.

It is plausible that despite the fact that we have turned off the vector-meson field at the saturation point, the diquark interaction induces enough repulsion to stabilize matter. In other words, in our model diquarks play the role of the vector-meson in the deconfined phase and the rearrangement of quarks from packages of three quarks to packages of two quarks is essential. In a quark exchange model of NN-interaction, the s-channel picture of quark exchange looks like two remaining diquark cores and a diquark in between. Therefore, one could say that the diquark picture is dual to a meson exchange picture. The bosonic approach reproduces the correct saturation point and a soft EoS. In fact, repulsive bosons are easier to handle than fermions where the correlated wave function cannot be adequately described by the mean-field theory. Moreover, the diquark BEC goes over directly into BCS-condensate.

In Fig. 8, we show the energy per baryon $\varepsilon_{h,q}/\rho_b$ as a function of inverse baryonic density $(\rho_b/\rho_0)^{-1}$ for two parameter sets given in tables 1 and 3. They exhibit a typical Van der Waals-like isotherm diagram where liquid and gaseous phases coexist. At low density in the confined region, nuclear matter is mechanically unstable since the pressure is negative. But the pressure in vacuum and at saturation density ρ_0 is equal to zero. Therefore, the nuclear matter mechanical instability can be prevented by fragmenting nuclear matter into droplets of nuclei, where each droplet has pressure zero and density equal to $\rho_0 = 0.15 \text{ fm}^{-3}$. Diquark BEC matter also breaks up into stable droplets in which the pressure is zero and density is ρ_b^d . The diquark BEC droplets are therefore surrounded by non-perturbative vacuum and droplets of nucleons. As we already discussed at the chemical potential $\mu_b = 923.25 \text{ MeV}$ chiral symmetry is restored. Therefore, diquark droplets exhibit QCD-matter in a chirally restored form, whereas the chiral symmetry within nucleonic droplets

⁶ A computation of the compression modulus of the joined nuclear-diquark EoS (solid and dashed lines in Fig. 7) exactly at the saturation point is not possible, since we have assumed a sharp boundary between the baryonic and the diquark phases.

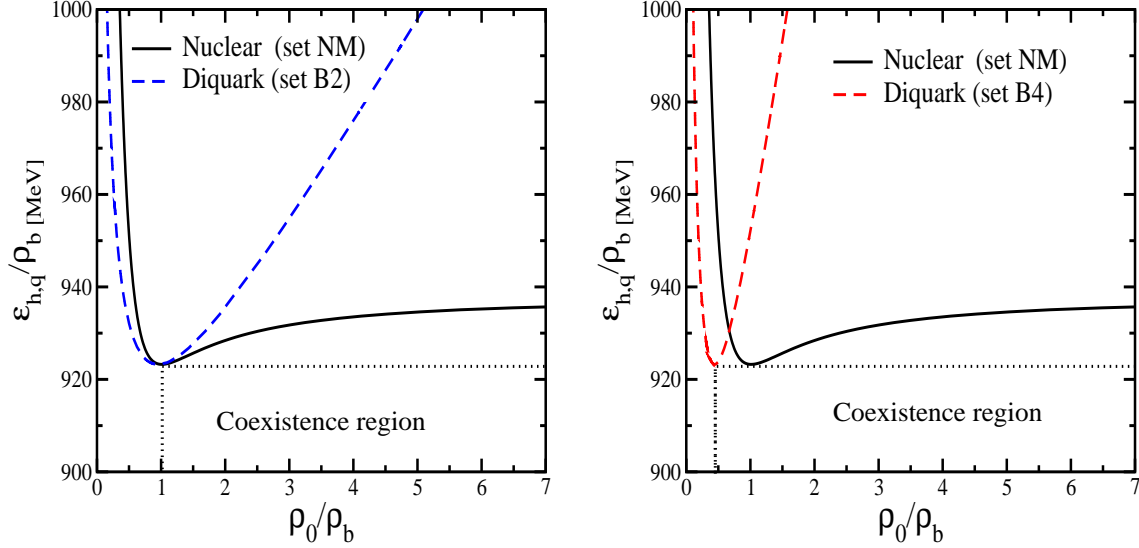


Fig. 8. Energy per baryon number as functions of inverse baryonic density $(\rho_b/\rho_0)^{-1}$ in the unit of the nuclear matter density ρ_0 . Various parameter sets given in tables 1 and 3 are used. The dotted line represents the Maxwell-construction which determines the region of coexistence: between the nucleons gas, hadronic droplets with $\bar{\sigma} \neq 0$, the droplets of diquark Bose-Einstein condensate with $\bar{\sigma} = 0$ surrounded by a non-trivial vacuum with $\bar{\sigma} = 93$ MeV.

is only partially restored. The nucleon mass at the saturation density is about 763 MeV for the parameter set NM, see Fig. 4. Therefore, in our scenario, multifragmentation has more facets than usually. It also signals a first order phase transition of chiral restoration and deconfinement. Ordinary nuclear matter can then be identified as being in the mixed phase of the first order phase transition: consisting of droplets of diquarks and droplets of nucleons surrounded by empty space.

Within this model we cannot directly identify the diquark BEC droplets with abnormal nuclei, since color should be gauged if the model is to yield color-singlet droplets. However, one may tempt to do so, since we know that within nucleons the chiral symmetry is already restored, and the quark density is not zero. In this case, one arrives at a similar picture to that in the MIT bag model. A similar picture of a nucleon as a bag within which chiral symmetry is restored has also been proposed by Buballa [30], Alford, Rajagopal and Wilczek [11] and Berges and Rajagopal [12], (see also Ref. [31]), but within quite different models and mechanisms. Note that here we can easily choose parameter sets where baryon density in droplets of diquarks is different from the nucleonic droplet $\rho_b^d \neq \rho_0$. Identifying a diquark droplet with abnormal nuclei is possible for $\rho_{b1} > \rho_0$, this may favor a soft EoS, see Fig. 6. In this picture, it is also possible to have combined droplets of nuclei and diquarks. A fraction of baryonic charge can then be delocalized in form of a diquark BEC. In this case, diquark concentration within nuclei can be smaller than nuclear matter density ρ_0 . A possible chemistry of such a mixed matter is beyond the

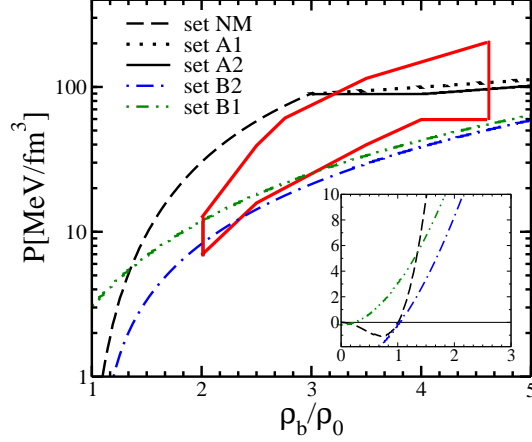


Fig. 9. Pressure as functions of ρ_b/ρ_0 for various parameter sets given in tables 1 and 3. Parameter sets A1 and A2 (table 2) are given with the assumption that the deconfinement takes place at $\mu^* = 1214.5$ MeV, corresponding to baryonic density $\rho_b^h/\rho_0 = 3$. Parameter set A2 leads to a coexistence region between nuclear and chirally restored diquark BEC matter within $3 \leq \rho_b/\rho_0 \leq 4$. Parameter sets B1 and B2 (table 3) are given with the assumption that the deconfinement takes place right at the nuclear matter saturation point $\mu_b^* = 923.25$ MeV. The gray closed line corresponds to the Danielewicz *et al.* constraint [29].

scope of this paper.

There are some experimental restrictions coming from the flow analysis in heavy-ion collisions which indicates the preferable theoretical values of pressure in a portion of baryonic density $2 < \rho_b/\rho_0 < 4.6$ at zero temperature [29]. This region is shown in Fig. 9 with a gray closed line. It is important to note that no single EoS can simultaneously describe all phenomenological data [29]. The area of allowed values does not represent experimental values itself but results from transport calculations for the motions of nucleons in a collision for a given EoS. To compare with the flow constraint region, we separate regions of SIS ($\rho_b < 3\rho_0$) and AGS ($\rho_b > 3\rho_0$) energies as weak and strong flow constraints. In this figure, we show the EoS we obtained for two cases of early deconfinement (sets B1 and B2 in table 3) and late deconfinement (sets A1 and A2). In both cases, the produced equations of state pass through the acceptable phenomenological region. For the region $\rho_b < 3\rho_0$ the EoS obtained by assuming rather early deconfinement (sets B1 and B2 in table 2) passes through the constraint region. These equations of state stay outside the acceptable phenomenological region at higher density. However, because of the diquark ultraviolet cutoff, at higher density of about $\rho_b > 2.6\rho_0$, the model is not trustworthy. The current available phenomenological data from heavy ion collisions cannot limit the acceptable boundaries on pressure as a function of density below two times the normal nuclear matter density [29]. Note that the models (for sets B1 and B2) assuming the deconfinement phase transition at relatively low baryonic density cannot be precluded by the present

flow constraint. This is in contrast with conclusion made in Ref. [29]. For the region $\rho_b > 3\rho_0$ the EoS obtained by assuming late deconfinement passes through the allowed region. For parameter sets A1 and A2, we assumed that the deconfinement takes place at baryonic density $\rho_b = 3\rho_0$. For parameter set A2, the deconfinement phase transition is first-order and it leads to a co-existence region between nuclear and chirally restored diquark BEC matter within $3 < \rho_b/\rho_0 < 4$. For parameter set A1, the deconfinement phase transition is second-order and there is no coexistence region. Note that since we used rather stiff EoS for the hadronic side (set NM), in the confined region the nuclear matter EoS stays outside allowed region. This is a general problem of these simple mean-field models and may be improved by adding further meson interactions or potential terms to the Lagrangian [23].

6 Summary and conclusions

In this paper, we investigated the nuclear matter and its possible phase transition to diquark BEC matter at zero temperature. For the hadronic phase we used a linear $\sigma - \omega$ model incorporating explicitly the effect of Dirac-sea. For the deconfined phase, we used a complex scalar field theory in terms of diquarks which couple to mesonic fields and repel each other. Nucleon, meson and diquark masses are dynamically generated via spontaneous symmetry breaking.

Our simplified theory does not yet give uniquely the order of a possible deconfinement transition, nor its location. However, as pointed out, there are indications which suggest that it might be first order and takes places above nuclear matter saturation density. In this paper, we studied the implication of different choices for the critical deconfinement chemical potential. Our knowledge about the form of matter above deconfinement is still very rudimentary. In this paper, we studied a possible formation of a diquark BEC phase with deconfinement and investigated its implication for the baryonic matter. Since we do not know the strength of the diquark-diquark interaction coupling g , we investigated possible values for this coupling and possible physical consequences.

We found that it is possible that nuclear matter undergoes a diquark BEC phase transition. Our study generally indicates the importance of the diquark BEC phenomenon at a rather low chemical potential. It has been shown within various models that phase transition from hadronic matter to normal quark matter cannot occur [13,33]. Based on our studies, deconfinement to diquark BEC matter seems to be a viable option.

We showed that chiral phase transition is of first order and coincides with

deconfinement transition. The compressibility of the EoS depends on the diquark-diquark coupling and the critical deconfinement chemical potential. We found that an early deconfinement and a weaker diquark-diquark interaction (or a stronger diquark BEC) soften the EoS. Assuming that deconfinement already takes place at saturation, we proposed a scenario in which the saturation properties can be described by the diquark BEC phenomenon. In contrast to the standard picture, the vector-meson is not needed and the diquark-diquark interactions provide enough repulsion in order to prevent the collapse of the system. The EoS obtained in this way are rather soft.

In particular, we studied the various coexistence patterns which may emerge if deconfinement takes place at different critical chemical potential. We showed if deconfinement takes place at higher baryonic chemical potential, due to a first-order phase transition there exists a coexistence region between the hadronic and the diquark matter. The extension of this region in density depends on the diquark interaction, a weaker diquark-diquark interaction widens this region. For model parameters with heavy diquark in vacuum (albeit within baryons), phase transition to diquark matter becomes of second-order. We also showed that if deconfinement takes place at about the nuclear matter saturation chemical potential, the ordinary nuclear matter can then be conceived as being in the mixed phase of the first order phase transition, consisting of droplets of nucleons and droplets of chirally restored BEC diquarks surrounded by a non-perturbative vacuum.

Diquark Bose-Einstein condensation guarantees a substantial presence of diquarks in the plasma. A heavy quark-antiquark pair ($Q\bar{Q}$) may be converted into a heavy baryon (Q -diquark) and exotic unstable pentaquark (\bar{Q} -diquark-diquark) in the presence of the diquark BEC. Also the ratio of Λ_c/Σ_c can be altered in presence of the diquark BEC, since Λ_c contains a scalar diquark while the production of Σ_c remains unaffected by the presence of the scalar diquarks [34]. It will be challenging for incoming facility at GSI/FAIR to probe a possible signature for the diquark BEC matter. Moreover, the diquark BEC may alter the compact star cooling behaviour. In principle, two quarks can be converted into a diquark and a pair of neutrinos via the following weak interaction process $u + d \rightarrow [ud]_{\text{diquark}} + \bar{\nu}_e + \nu_e$. These extra neutrinos will be strongly enhanced in the presence of the diquark BEC. This mechanism accelerates the cooling of compact star. On the other hand, it has been shown that the cooling process will be suppressed in the presence of BCS-pairing [35]. Therefore, the cooling behaviour of compact star may provide a possible signature of existence of the diquark BEC matter and BEC-BCS crossover.

It is highly desirable to improve our knowledge about the nature of diquark interaction in medium and its possible connections to QCD parameters or some phenomenological inputs. It is also of interest to investigate the implication of the nuclear-diquark model presented here under neutron stars conditions.

Acknowledgements

A.H.R. would like to thank I. A. Shovkovy for very fruitful discussions and acknowledges the financial support from the Alexander von Humboldt foundation.

References

- [1] J. B. Kogut *et. al.*, Phys. Rev. Lett. **50**, 393 (1983); F. Karsch and E. Laermann, Phys. Rev. **D50**, 6954 (1994); F. Karsch, E. Laermann and A. Peikert, Nucl. Phys. **B605**, 579 (2001).
- [2] O. Philipsen, PoS **LAT2005**, 016 (2005), [hep-lat/0510077].
- [3] M. A. Halasz, A. D. Jackson, R. E. Shrock, M. A. Stephanov, J. J. M. Verbaarschot, Phys. Rev. **D58**, 096007 (1998).
- [4] K. Rajagopal and F. Wilczek, hep-ph/0011333; M. G. Alford, Ann. Rev. Nucl. Part. Sci. **51**, 131 (2001), [hep-ph/0102047].
- [5] N. Kaiser, S. Fritsch and W. Weise, Nucl. Phys. **A697**, 255 (2002).
- [6] D. H. Rischke, D. T. Son and M. A. Stephanov, Phys. Rev. Lett. **87**, 062001 (2001).
- [7] M. Anselmino *et. al.*, Rev. Mod. Phys. **65**, 1199 (1993); F. Wilczek, hep-ph/0409168.
- [8] For example: T. Schafer, E. V. Shuryak and J. J. M. Verbaarschot, Nucl. Phys. **B412** 143 (1994), [hep-ph/9306220]; A. Buck, R. Alkofer, H. Reinhardt, Phys. Lett. **B286**, 29 (1992); N. Ishii, W. Bentz, K. Yazaki, Nucl. Phys. **A587**, 617 (1995); A. H. Rezaeian, N. R. Walet and M. C. Birse, Phys. Rev. **C70**, 065203 (2004), [hep-ph/0408233]; A. H. Rezaeian, hep-ph/0507304 (and references therein); M. Oettel, G. Hellstern, R. Alkofer and H. Reinhardt, Phys. Rev. **C58**, 2459 (1998), [nucl-th/9805054].
- [9] A. H. Rezaeian and H. J. Pirner, Nucl. Phys. **A769**, 35 (2006), [nucl-th/0510041].
- [10] W. Bentz and A. W. Thomas, Nucl. Phys. **A696**, 138 (2001), [nucl-th/0105022].
- [11] M. Alford, K. Rajagopal and F. Wilczek, Phys. Lett. **B422**, 247 (1998), [hep-ph/9711395].
- [12] J. Berges and K. Rajagopal, Nucl. Phys. **B538**, 215 (1999), [hep-ph/9804233].
- [13] M. Buballa, Phys. Rept. **407**, 205 (2005), [hep-ph/0402234].
- [14] D. H. Rischke, Prog. Part. Nucl. Phys. **52**, 197 (2004), [nucl-th/0305030]; I. A. Shovkovy, Found. Phys. **35**, 1309 (2005), [nucl-th/0410091].

- [15] For example: C. A. Regal, M. Greiner, and D. S. Jin, Phys. Rev. Lett. **92**, 040403 (2004).
- [16] M. Matsuzaki, Phys. Rev. **D62**, 017501 (2000), [hep-ph/9910541]; E. Babaev, Int. J. Mod. Phys. **A16**, 1175 (2002), [hep-th/9909052]; M. Kitazawa, T. Koide, T. Kunihiro and Y. Nemoto, Phys. Rev. **D65**, 091504 (2002), [nucl-th/0111022]; H. Abuki, T. Hasuda and K. Itakura, Phys. Rev. **D65**, 074014 (2002), [hep-ph/0109013]; M. Kitazawa, T. Koide, T. Kunihiro and Y. Nemoto, Phys. Rev. **D70**, 056003 (2004), [hep-ph/0309026]; Y. Nishida and H. Abuki, Phys. Rev. **D72**, 096004 (2005), [hep-ph/0504083]; M. Kitazawa, T. Koide, T. Kunihiro and Y. Nemoto, Prog. Theor. Phys. **114**, 117 (2005); K. Nawa, E. Nakano and H. Yabu, hep-ph/0509029; H. Abuki, hep-ph/0605081.
- [17] J. F. Donoghue and K. S. Sateesh, Phys. Rev. **D38**, 360 (1988); D. Kastor and J. H. Traschen, Phys. Rev. **D44**, 3791 (1991); J. E. Horvath, J. A. de Freitas Pacheco and J. C. N. de Araujo, Phys. Rev. **D46**, 4754 (1992).
- [18] V. A. Miransky and I. A. Shovkovy, Phys. Rev. Lett. **88**, 111601 (2002); T. Schaefer, D. T. Son, M. A. Stephanov, D. Toublan and J. J. M. Verbaarschot, Phys. Lett. **B522**, 67 (2001); D. Blaschke, D. Ebert, K. G. Klimenko, M. K. Volkov and V. L. Yudichev, Phys. Rev. **D70**, 014006 (2004).
- [19] H. B. Nielsen and S. Chadha, Nucl. Phys. **B105**, 445 (1976).
- [20] E. M. Lifshitz and L.P. Pitaevskii, *Statistical Physics, Part 2*, (Pergamon, 1980).
- [21] R. J. Furnstahl, B. D. Serot and H.-B. Tang, Nucl. Phys. **A618**, 446 (1997).
- [22] A. Manohar and H. Georgi, Nucl. Phys. **B234**, 189 (1984).
- [23] B. D. Serot and J. D. Walecka, Int. J. Mod. Phys. **E6**, 515 (1997).
- [24] A. H. Rezaeian, nucl-th/0512027.
- [25] V. Koch, T. S. Biro, J. Kunz and U. Mosel, Phys. Lett. **B185**, 1 (1987); T. J. Burvenich and D. G. Madland, Nucl. Phys. **A729**, 769 (2003).
- [26] J. Boguta, Phys. Lett. **B120**, 34 (1983); **128B**, 19 (1983).
- [27] M. Hess, F. Karsch, E. Laermann and I. Wetzorke, Phys. Rev. **D58**, 111502 (1998).
- [28] J. P. Blaizot, Phys. Rept. **64**, 171 (1980); J. Piekarewicz, Phys. Rev. **C69**, 041301 (2004).
- [29] P. Danielewicz, R. Lacey and W. G. Lynch, Science **298**, 1592 (2002).
- [30] M. Buballa, Nucl. Phys. **A611**, 393 (1996).
- [31] T. M. Schwarz, S. P. Klevansky and G. Papp, Phys. Rev. **C60**, 055205 (1999).
- [32] P. de Forcrand and S. Kratochvila, Nucl. Phys. (Proc. Suppl.) **B153**, 62 (2006), [hep-lat/0602024]; S. Kratochvila and P. de Forcrand, PoS **LAT2005**, 167 (2006), [hep-lat/0509143].

- [33] For example: I. N. Mishustin, L. M. Satarov, H. Stoecker and W. Greiner, Phys. Rev. **C66**, 015202 (2002).
- [34] K. S. Sateesh, Phys. Rev. **D45**, 866 (1992).
- [35] For example: M. G. Alford, J. A. Bowers and K. Rajagopal, J. Phys. **G27**, 541 (2001), [hep-ph/0009357].